

Engineering an anisotropic Dicke model of Rydberg atom arrays in an optical cavity with dipole–dipole interactions

Bao-Yun Dong(董保云), Yanhua Zhou(周彦桦), Wei Wang(王伟), and Tao Wang(汪涛)
Citation: Chin. Phys. B, 2025, 34 (**11**): 114203. DOI: 10.1088/1674-1056/ade388
http://cpb.iphy.ac.cn; http://iopscience.iop.org/cpb

What follows is a list of articles you may be interested in

Room-temperature exciton-polariton condensation in pressed perovskite microcavities

Tianyin Zhu(朱天寅), Zelei Chen(陈泽磊), Xiaoyu Wang(王小宇), Zhongmin Huang(黄钟民), Haibin Zhao(赵海斌), and Jun Wang(王俊)
Chin. Phys. B, 2025, 34 (**9**): 094202. DOI: 10.1088/1674-1056/addce6

Quantitative determination of modal photon number density spectrum in arbitrary dielectric structures with a quantum emitter

Li-Heng Chen(陈立恒), Fengfeng Luo(罗凤凤), and Yonggui Gao(高勇贵)
Chin. Phys. B, 2025, 34 (**4**): 044204. DOI: 10.1088/1674-1056/adb262

Effective Hamiltonian of the Jaynes-Cummings model beyond rotating-wave approximation

Yi-Fan Wang(王伊凡), Hong-Hao Yin(尹洪浩), Ming-Yue Yang(杨明月), An-Chun Ji(纪安春), and Qing Sun(孙青)
Chin. Phys. B, 2021, 30 (**6**): 064204. DOI: 10.1088/1674-1056/abd930

Extraordinary propagation characteristics of electromagnetic waves in one-dimensional anti-*PT*-symmetric ring optical waveguide network

Jie-Feng Xu(许杰锋), Xiang-Bo Yang(杨湘波), Hao-Han Chen(陈浩瀚), Zhan-Hong Lin(林展鸿)
Chin. Phys. B, 2020, 29 (**6**): 064201. DOI: 10.1088/1674-1056/ab8371

Multi-level effects in the high-order harmonic generation driven by intense frequency-comb laser fields

Zhao Di (赵迪), Jiang Chen-Wei (蒋臣威), Li Fu-Li (李福利)
Chin. Phys. B, 2015, 24 (**7**): 074205. DOI: 10.1088/1674-1056/24/7/074205

Engineering an anisotropic Dicke model of Rydberg atom arrays in an optical cavity with dipole–dipole interactions

Bao-Yun Dong(董保云)[1,2], Yanhua Zhou(周彦桦)[3,4], Wei Wang(王伟)[1,2,†], and Tao Wang(汪涛)[1,2,‡]

[1] *Department of Physics, and Chongqing Key Laboratory for Strongly Coupled Physics, Chongqing University, Chongqing* 401331, *China*
[2] *Center of Modern Physics, Institute for Smart City of Chongqing University in Liyang, Liyang* 213300, *China*
[3] *National Time Service Center, Chinese Academy of Sciences, Xi'an* 710600, *China*
[4] *School of Astronomy and Space Science, University of Chinese Academy of Sciences, Beijing* 100049, *China*

(Received 17 April 2025; revised manuscript received 26 May 2025; accepted manuscript online 11 June 2025)

The anisotropic Dicke model offers a platform for the exploration of numerous quantum many-body phenomena. Here, we propose a Floquet-engineered scheme to realize such a system with strong dipole–dipole interactions using Rydberg atom arrays in an optical cavity. By periodically modulating the microwave fields, the anisotropic parameter can be precisely controlled and tuned between zero and one, enabling the system to transition smoothly from being purely dominated by rotating-wave terms to being exclusively governed by counter- rotating wave excitations. Leveraging this tunability, we demonstrate enhanced preparation of adiabatic superradiant and superradiant solid phases where symmetry-protected energy gaps suppress undesired level crossings. Our approach, combining Rydberg interactions and cavity-mediated long-range correlations, establishes a versatile framework for the quantum simulation of light–matter interactions and the exploration of exotic many-body phases.

Keywords: anisotropic Dicke model, Floquet, Rydberg atom arrays, adiabatic state preparation, superradiant solid phases

PACS: 42.50.Pq, 32.80.Ee, 05.30.Rt

DOI: 10.1088/1674-1056/ade388 **CSTR:** 32038.14.CPB.ade388

1. Introduction

As one of the correlated many-body systems, the light–matter interaction problem has attracted considerable attention and has been actively investigated over many decades.[1,2] Researchers wish to to capture the underlying physics of such issues. The Dicke model was proposed in 1954 by Dicke[3] and describes a large number of two-level atoms coupled to a single mode of a quantized radiation field. When the coupling strength is much smaller than the mode frequency, a simplified scenario can be used. If we neglect the counter-rotating wave (CRW) terms, the reduced Tavis–Cummings model[4–8] exhibits excitation number conservation. On the other hand, if the rotating-wave approximation (RWA)[9] fails and the system reaches the strong coupling regime,[10–13] the full quantum Dicke model[14–19] is necessary. In few-body systems, investigations of the CRW terms have shown that many interesting quantum effects[20–26] can be induced, such as the preparation of nonclassical states,[27] three-photon resonance,[28] the deterioration of the photon blockade effect,[29,30] and so on.

Recently, the generalized Dicke model, named the anisotropic Dicke model (ADM),[31–34] has sparked considerable research interest. Its noteworthy feature is its use of different coupling strengths for the RW and CRW terms. Because of its intriguing properties, it has been employed to investigate a range of theoretical topics, including quantum phase transitions,[35,36] critical behaviors,[36] and Floquet heating.[37] For example, exciting research results indicate that the ADM exhibits not only a phase transition from the normal phase to the superradiant (SR) phase but also ergodic to non-ergodic transitions.[38] It is notable that the observation of the intriguing physical phenomena of the ADM largely relies on the tunability of the CRW terms. Moreover, the high controllability of the coupling strengths of the RW and CRW terms assists in observing the effects of the pure CRW terms. However, an open question remains, namely, how to engineer the tunability in real experiments.

Quantum simulation utilizes controlled quantum systems to model complex physical phenomena that are intractable classically, aiming to explore quantum many-body problems.[39–41] Among these simulators, Rydberg atoms offer a unique experimental platform due to their advantages in scalability, coherence time, and strong, tunable interactions.[42–46] Placing the atomic ensemble within an optical cavity allows long-range interactions to take place between the atoms and the cavity, making it possible to create multipartite entanglements and observe collective phenomena.[47–52] Recent advances in the programmable manipulation of isolated systems have enabled detailed studies

†Corresponding author. E-mail: weiwangphys@163.com
‡Corresponding author. E-mail: tauwaang@cqu.edu.cn

© 2025 Chinese Physical Society and IOP Publishing Ltd. All rights, including for text and data mining, AI training, and similar technologies, are reserved.

of equilibrium and nonequilibrium states under strong matter–matter interactions.[53–56] Remarkably, investigating quantum adiabatic evolution is a promising way to observe quantum many-body dynamics[57] and solve combinatorial optimization problems.[58,59] It is thus the next step in investigating the interplay between strong light–atom and atom–atom interactions,[60,61] which represents a significant advancement in simulating and understanding related many-body problems of quantum matter and light.

In this paper, we propose to realize an anisotropic Dicke model and Floquet engineer its CRW in the context of Rydberg array simulations. Specifically, by designing an appropriate two-photon process of three-level atoms, we derive an effective two-level Hamiltonian incorporated into the strong atom-interaction ADM. Light–atom coupling is capable of reaching both the strong and ultrastrong coupling regimes in ultrafine optical cavities. We further show that the tunability of the CRW can be engineered by modulating a microwave field. As an application of this controllability, we demonstrate that tuning the coupled resonator waveguide (CRW) via the microwave field allows us to control the eigenenergy distribution, facilitating the preparation of adiabatic superradiant (SR) and superradiant solid (SRS) states. Here, the SRS phase is novelly characterized by the coexistence of solid and SR orders and has been predicted due to the competition between the nearest-neighbor Rydberg blockade and the long-range exchange interactions mediated by the photon.[62–64] The SRS phase provides the necessary conditions for the study of related physical phases.

The remainder of this paper is organized as follows. Section 2 first introduces the theoretical model and our derived scheme. We then derive the effective anisotropic Dicke Hamiltonian and discuss its tunability. Section 3 is dedicated to analyzing the impact of controllable strong CRW terms on their adiabatic evolution, which is demonstrated for the SR and SRS phases, Finally, in Section 4, we conclude with a discussion.

2. Floquet engineering the effective Hamiltonian

We discuss cold Rydberg atoms trapped by optical tweezers in a geometry that forms a one-dimensional chain or a two-dimensional square lattice. Placed inside an ultrafine optical cavity, the atoms are further assumed to couple to the cavity photon and the beam of a classical laser, as schematically depicted in Fig. 1(a). Considering each atom at the antinode of the cavity mode, the atomic ground states $|g\rangle$ and the intermediate states $|m\rangle$ are coupled by a single quantized cavity mode with strength Ω_1. The detuning is $\Delta_1 = \omega_l - \omega_C$, where ω_C is the frequency of the cavity mode and ω_l is the frequency difference between $|g\rangle$ and $|m\rangle$. A classical laser field of frequency ω_p non-resonantly drives the transition of $|m\rangle \to |e\rangle$ with the Rabi frequency Ω_2. If ω_2 denotes the frequency difference between $|m\rangle$ and $|e\rangle$, the detuning is $\Delta_2 = \omega_2 - \omega_p$. The above two-photon process is shown in Fig. 1(b), where the total detuning is $\Delta = \Delta_1 + \Delta_2$. Omitting atomic external motions and setting $\hbar = 1$, one can describe the dynamics using the following Hamiltonian:

$$H_E = H_D + H_I. \tag{1}$$

The diagonal term H_D and the interaction terms H_I are correspondingly given by

$$\begin{aligned} H_D &= \omega_C a^\dagger a + \omega_l \sum_{j=1}^{N} |m_j\rangle\langle m_j| + (\omega_l + \omega_2) \sum_{j=1}^{N} |e_j\rangle\langle e_j| \\ &\quad + V \sum_{\langle j,k\rangle} |e_j\rangle\langle e_j|e_k\rangle\langle e_k|, \end{aligned} \tag{2}$$

$$\begin{aligned} H_I &= \frac{\Omega_1}{\sqrt{N}}(a^\dagger + a) \sum_{j=1}^{N} (|m_j\rangle\langle g_j| + |g_j\rangle\langle m_j|) \\ &\quad + \frac{\Omega_2 \cos(\omega_p t)}{\sqrt{N}} \sum_{j=1}^{N} (|m_j\rangle\langle e_j| + |e_j\rangle\langle m_j|). \end{aligned} \tag{3}$$

Here, $a^\dagger$ (a) is the creation (annihilation) operator of photons in the cavity. The nearest-neighbor dipole–dipole interaction of the Rydberg state with strength V is considered here. The subscript $\langle j,k\rangle$ of the summation symbol $\sum$ indicates that the summation is performed over nearest-neighbor pairs once. N is the total number of atoms trapped by optical tweezers. The maximum occupation number of atoms in each site should be one because of the Rydberg blockade.

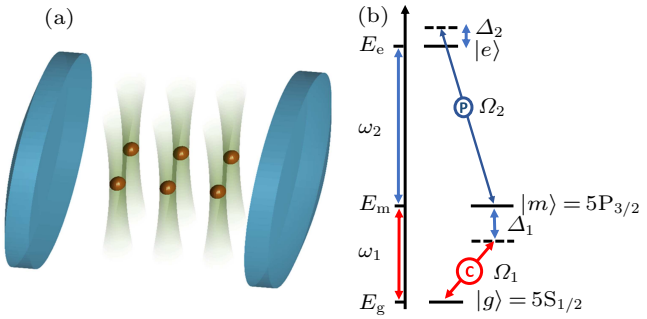


Fig. 1. (a) Schematic diagram of Rydberg atoms trapped by square lattice optical tweezers, which interact with an ultrafine optical cavity. Each array site is occupied by a single atom and located at an antinode of the cavity mode. (b) Illustration of atomic energy levels and the associated two-photon pathway. The cavity mode excites rubidium atomic ground states $5S_{1/2}$ to intermediate states $5P_{3/2}$. The states $5P_{3/2}$ are coupled to the Rydberg state $|e\rangle$ by a classic laser beam. After driven microwave fields are introduced and intermediate states are removed, the two-photon processes, assisted by Floquet photons, give rise to modulated coupling between photons and two-level atoms.

To deepen our understanding of the CRW terms, hereafter we Floquet engineer the Hamiltonian. To be specific, we apply a microwave beam $E(t) = E_A \sin(\omega_s t/2)$ to the system, where E_A and ω_s are the amplitude and frequency of the microwaves, respectively.[65,66] Due to the AC Stark effect, there is an equivalent potential $A\cos(\omega_s t)$ on the Rydberg states

such that $A \propto E_{\rm A}^2$ is the amplitude of the potential. Therefore, the Hamiltonian of the diagonal part is modified to read

$$\begin{aligned} H_{\rm Dri} &= \omega_{\rm C} a^\dagger a + \omega_{\rm l} \sum_{j=1}^{N} |m_j\rangle\langle m_j| + V \sum_{\langle j,k\rangle} |e_j\rangle\langle e_j|e_k\rangle\langle e_k| \\ &\quad + [\omega_{\rm l} + \omega_2 + A\cos(\omega_{\rm s} t)] \sum_{j=1}^{N} |e_j\rangle\langle e_j|. \end{aligned} \tag{4}$$

In order to deal with the time-dependent terms in Eq. (3), we implement a unitary transformation using the operator $u = \exp\{\sum_{j=1}^{N}(-{\rm i}|e_j\rangle\langle e_j|\omega_{\rm p} t)\}$. After we apply the RWA to the interaction between the classical laser and the atoms, the Hamiltonian becomes

$$\begin{aligned} H_{\rm DR} &= \omega_{\rm C} a^\dagger a + \omega_{\rm l} \sum_{j=1}^{N} |m_j\rangle\langle m_j| + V \sum_{\langle j,k\rangle} |e_j\rangle\langle e_j|e_k\rangle\langle e_k| \\ &\quad + [\omega_{\rm l} + \Delta_2 + A\cos(\omega_{\rm s} t)] \sum_{j=1}^{N} |e_j\rangle\langle e_j|, \end{aligned} \tag{5}$$

$$\begin{aligned} H_{\rm IR} &= \frac{\Omega_1}{\sqrt{N}}(a^\dagger + a) \sum_{j=1}^{N} (|m_j\rangle\langle g_j| + |g_j\rangle\langle m_j|) \\ &\quad + \frac{\Omega_2}{\sqrt{N}} \sum_{j=1}^{N} (|m_j\rangle\langle e_j| + |e_j\rangle\langle m_j|). \end{aligned} \tag{6}$$

In a typical Rydberg experiment, taking ^{87}Rb atoms as an example, the intermediate states $5{\rm P}_{3/2}$ have a long lifetime (denoted by τ). Upon detuning the cavity mode such that $\Delta \approx 0$ and $\Delta_1 \gg \tau^{-1}$, the intermediate states can be regarded as unpopulated and can be eliminated to reduce the effective Hamiltonian. We follow the standard Schrieffer–Wolff transformation.[67] Since the periodic driving contributes zero to the shift of energy levels on average over a long period of time, we first construct an anti-Hermitian generator S based on the interaction Hamiltonian given in Eq. (6) for each site j, as follows:

$$S^j = \left(\frac{\Omega_1 a |m_j\rangle\langle g_j|}{\Delta_1} + \frac{\Omega_1 a^\dagger |m_j\rangle\langle g_j|}{\omega_{\rm l} + \omega_{\rm C}} - \frac{\Omega_2 |m_j\rangle\langle e_j|}{\Delta_2} \right) - {\rm h.c.}$$

After a second-order truncation, we obtain the subspace effective Hamiltonian $H_{\rm eff}^j = {\rm e}^S (H_{\rm DR}^j + H_{\rm IR}^j){\rm e}^{-S} = H_{\rm DR}^j + \frac{1}{2}[S^j, H_{\rm IR}^j]$, for which the commutation relation can be straightforwardly formulated as follows:

$$\left[S^j, H_{\rm IR}^j\right] = |\Omega_1|^2 |m_j\rangle\langle m_j| \left(\frac{2a^\dagger a}{\omega_{\rm l} + \omega_{\rm C}} + \frac{a^{\dagger 2}}{\omega_{\rm l} + \omega_{\rm C}} + \frac{a^{\dagger 2}}{\Delta_1} + \frac{a^2}{\Delta_1} + \frac{a^2}{\omega_{\rm l} + \omega_{\rm C}} + \frac{2aa^\dagger}{\Delta_1} \right) - \frac{2|\Omega_2|^2}{\Delta_2} |m_j\rangle\langle m_j| \tag{7}$$

$$- |\Omega_1|^2 |g_j\rangle\langle g_j| \left(\frac{2aa^\dagger}{\omega_{\rm l} + \omega_{\rm C}} + \frac{a^2}{\omega_{\rm l} + \omega_{\rm C}} + \frac{a^2}{\Delta_1} + \frac{a^{\dagger 2}}{\Delta_1} + \frac{a^{\dagger 2}}{\omega_{\rm l} + \omega_{\rm C}} + \frac{2a^\dagger a}{\Delta_1} \right) + \frac{2|\Omega_2|^2}{\Delta_2} |e_j\rangle\langle e_j| \tag{8}$$

$$+ \Omega_1^* \Omega_2 |g_j\rangle\langle e_j| \left(-\frac{a}{\omega_{\rm l} + \omega_{\rm C}} + \frac{a}{\Delta_2} - \frac{a^\dagger}{\Delta_1} + \frac{a^\dagger}{\Delta_2} \right) + \Omega_2^* \Omega_1 |e_j\rangle\langle g_j| \left(-\frac{a^\dagger}{\omega_{\rm l} + \omega_{\rm C}} + \frac{a^\dagger}{\Delta_2} - \frac{a}{\Delta_1} + \frac{a}{\Delta_2} \right). \tag{9}$$

We now proceed to discuss a simpler result in which one only cares about atomic dynamics in this type of atom–photon interaction. In this case, we drop Eqs. (7) and (8) because these second-order photon interactions only modify the energy levels of atomic states. For the remaining terms in Eq. (9), it is clear that the intermediate state is decoupled from the ground state and the Rydberg state. Thus, the projection operators are rewritten using the on-site fundamental bosonic operators: $\sigma_j^z = (|e_j\rangle\langle e_j| - |g_j\rangle\langle g_j|)$, $\sigma_j^+ = |e_j\rangle\langle g_j|$, and $\sigma_j^- = |g_j\rangle\langle e_j|$. Additionally, using $n_i = (1 + \sigma_i^z)/2$, $\omega_{\rm A} = \omega_{\rm l} + \Delta_2$, the single-particle effective Hamiltonian can be expressed as a two-level system

$$\begin{aligned} H_{\rm eff}^j &= \omega_{\rm C} a^\dagger a + [\omega_{\rm A} + A\cos(\omega_{\rm s} t)] n_j \\ &\quad + \left(\Omega_{\rm e1} a \sigma_j^+ + \Omega_{\rm e2} a^\dagger \sigma_j^+ + {\rm h.c.} \right). \end{aligned} \tag{10}$$

Note that since $\omega_{\rm l}$ and $\omega_{\rm C}$ can be in the hundreds of terahertz range in rubidium atom experiments, we neglect $\frac{1}{\omega_{\rm l} + \omega_{\rm C}}$. We then define the CRW and RW effective coupling strengths as $\Omega_{\rm e1} = \frac{\Omega_2^* \Omega_1}{2}\left(\frac{1}{\Delta_2} - \frac{1}{\Delta_1}\right)$ and $\Omega_{\rm e2} = \frac{\Omega_2^* \Omega_1}{2}\frac{1}{\Delta_2}$, respectively.

We now turn to a discussion of the properties of the effective Hamiltonian. It is useful to rewrite the full effective Hamiltonian

$$\begin{aligned} H_{\rm eff} &= \omega_{\rm C} a^\dagger a + [\omega_{\rm A} + A\cos(\omega_{\rm s} t)] \sum_{j=1}^{N} n_j + V \sum_{\langle j,k\rangle} n_j n_k \\ &\quad + \sum_{j=1}^{N} \left(\frac{\Omega_{\rm e1}}{\sqrt{N}} a \sigma_j^+ + \frac{\Omega_{\rm e2}}{\sqrt{N}} a^\dagger \sigma_j^+ + {\rm h.c.} \right). \end{aligned} \tag{11}$$

Here, we face a similar time-dependent periodic issue to that in Eq. (4). Following the same procedure, we first apply the unitary transformation

$$U_1 = \exp\left\{ -{\rm i}\omega_{\rm C} a^\dagger a t - {\rm i}\left[\omega_{\rm A} t + \frac{A}{\omega_{\rm s}} \sin(\omega_{\rm s} t) \right] \sum_{j=1}^{N} n_j \right\},$$

under which the Hamiltonian becomes

$$\begin{aligned} \widetilde{H}_{\rm E} &= V \sum_{\langle j,k\rangle} n_j n_k + \frac{\Omega_{\rm e1}}{\sqrt{N}} \sum_{j=1}^{N} \left\{ W_1(t) a \sigma_j^+ + {\rm h.c.} \right\} \\ &\quad + \frac{\Omega_{\rm e2}}{\sqrt{N}} \sum_{j=1}^{N} \left\{ W_2(t) a^\dagger \sigma_j^+ + {\rm h.c.} \right\}. \end{aligned} \tag{12}$$

Here,

$$W_1(t) = \exp\left\{ {\rm i}\left[-\omega_{\rm C} t + \omega_{\rm A} t + \frac{A}{\omega_{\rm s}} \sin(\omega_{\rm s} t) \right] \right\},$$

$$W_2(t)=\exp\left\{\mathrm{i}\left[\omega_{\mathrm{C}}t+\omega_{\mathrm{A}}t+\frac{A}{\omega_{\mathrm{s}}}\sin(\omega_{\mathrm{s}}t)\right]\right\}.$$

Under the condition $|\omega_{\mathrm{A}}-n_t\omega_{\mathrm{s}}|\ll\omega_{\mathrm{s}}$, we adopt the resolved sideband approximation, which means that only the n_t-th sideband needs to be considered. Based on this consideration, we next transform the Hamiltonian Eq. (12) back using

$$U_2=\exp\left[\mathrm{i}\left(\omega_{\mathrm{C}}-n_t\omega_{\mathrm{s}}\right)a^{\dagger}at+\mathrm{i}\left(\omega_{\mathrm{A}}-n_t\omega_{\mathrm{s}}\right)t\sum_{j=1}^{N}n_j\right],$$

which leads to

$$\begin{aligned}H_{\mathrm{F}}=&\frac{\Omega_{\mathrm{e}1}}{\sqrt{N}}\sum_{j=1}^{N}\left\{\exp\left[\mathrm{i}\frac{A}{\omega_{\mathrm{s}}}\sin(\omega_{\mathrm{s}}t)\right]a\sigma_j^{+}+\mathrm{h.c.}\right\}\\&+\frac{\Omega_{\mathrm{e}2}}{\sqrt{N}}\sum_{j=1}^{N}\left\{\exp\left[\mathrm{i}\frac{A}{\omega_{\mathrm{s}}}\sin(\omega_{\mathrm{s}}t)+2\mathrm{i}n_t\omega_{\mathrm{s}}t\right]a^{\dagger}\sigma_j^{+}+\mathrm{h.c.}\right\}\\&+\left(\omega_{\mathrm{C}}-n_t\omega_{\mathrm{s}}\right)a^{\dagger}a+V\sum_{\langle j,k\rangle}n_jn_k+\left(\omega_{\mathrm{A}}-n_t\omega_{\mathrm{s}}\right)\sum_{j=1}^{N}n_j.\end{aligned}\tag{13}$$

Using the Jacobi–Anger relation

$$\mathrm{e}^{\mathrm{i}K\sin\omega_{\mathrm{s}}t}=\sum_{n=0}^{\infty}J_n[K]\,\mathrm{e}^{\mathrm{i}n\omega_{\mathrm{s}}t}$$

and the Floquet–Magnus expansion, we finally obtain the lowest-order effective Hamiltonian

$$\begin{aligned}H_{\mathrm{FM}}&=\frac{1}{T}\int_0^T H_{\mathrm{F}}\,\mathrm{d}t\\&=\left(\Omega_{\mathrm{e}3}\sum_{j=1}^{N}\sigma_j^{+}a+\Omega_{\mathrm{e}4}\sum_{j=1}^{N}\sigma_j^{+}a^{\dagger}+\mathrm{h.c.}\right)\\&\quad+\widetilde{\omega}_{\mathrm{C}}a^{\dagger}a+V\sum_{\langle j,k\rangle}n_jn_k+\widetilde{\omega}_{\mathrm{A}}\sum_{j=1}^{N}n_j,\end{aligned}\tag{14}$$

where

$$\Omega_{\mathrm{e}3}=\frac{\Omega_{\mathrm{e}1}}{\sqrt{N}}J_0\left[\frac{A}{\omega_{\mathrm{s}}}\right],\quad\Omega_{\mathrm{e}4}=\frac{\Omega_{\mathrm{e}2}}{\sqrt{N}}J_{2n_t}\left[\frac{A}{\omega_{\mathrm{s}}}\right],\tag{15}$$

$$\widetilde{\omega}_{\mathrm{C}}=\omega_{\mathrm{C}}-n_t\omega_{\mathrm{s}},\quad\widetilde{\omega}_{\mathrm{A}}=\omega_{\mathrm{A}}-n_t\omega_{\mathrm{s}}.\tag{16}$$

Note that because $\Omega_{\mathrm{e}1}$ and $\Omega_{\mathrm{e}2}$ in Eqs. (15) and (16) depend on the detunings of the two-photon process, which must meet some approximation conditions, it is difficult to regulate $\Omega_{\mathrm{e}3}$ and $\Omega_{\mathrm{e}4}$ through them. However, by introducing the Bessel function, our Floquet engineering scheme makes the control of the effective coupling strengths of RW and CRW possible. The numerical results demonstrating their tunability are shown in Fig. 2, where $\Omega_{\mathrm{e}1}=2$, $\Omega_{\mathrm{e}2}=1$, and $n_t=1$. For convenience in the following discussions, we let $\alpha=\frac{\Omega_{\mathrm{e}4}}{\Omega_{\mathrm{e}3}+\Omega_{\mathrm{e}4}}$, which is commonly referred to as the anisotropic parameter in the Rabi model and the Dicke model, while $\Omega=\Omega_{\mathrm{e}3}+\Omega_{\mathrm{e}4}$ is the total coupling strength of the atoms and the cavity field. Eq. (14) can now be rewritten as

$$\begin{aligned}H=&\widetilde{\omega}_{\mathrm{C}}a^{\dagger}a+(1-\alpha)\frac{\Omega}{\sqrt{N}}\sum_{j=1}^{N}(\sigma_j^{+}a+a^{\dagger}\sigma_j^{-})\\&+\alpha\frac{\Omega}{\sqrt{N}}\sum_{j=1}^{N}(\sigma_j^{+}a^{\dagger}+a\sigma_j^{-})\\&+V\sum_{\langle j,k\rangle}n_jn_k+\widetilde{\omega}_{\mathrm{A}}\sum_{j=1}^{N}n_j.\end{aligned}\tag{17}$$

For $V=0$, Eq. (17) reduces to the ADM, where the critical point of the phase transition from the normal phase to the SR phase, $\Omega=\sqrt{\widetilde{\omega}_{\mathrm{C}}\widetilde{\omega}_{\mathrm{A}}}$, is independent of α.[32,37] When the Rydberg dipole–dipole interaction is incorporated but $\alpha=0$, previous research has demonstrated a quantum phase transition in both one-dimensional and square arrays and even discovered a novel phase, the SRS phase, which breaks $U(1)$ and translation symmetries simultaneously.[62,63] The SRS phase is equivalent to the Ising–Dicke model for $\alpha=0.5$. In addition to the observation of quantum phase transitions,[61,68] meson oscillations in the spin states, and the squeezed-vacuum light state,[60] some such results can find applications in enhancing the measurement sensitivity of temperatures and external fields.[69]

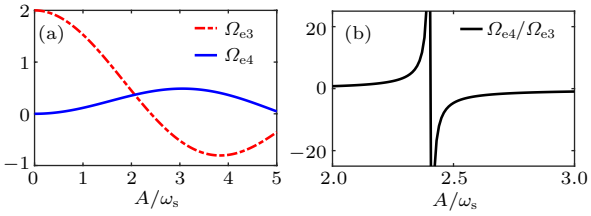


Fig. 2. (a) The coupling strengths of RW and CRW versus the ratio of driving amplitude to frequency, denoted by the blue solid line and the red dot-dashed line, respectively. (b) The ratio of the coupling strength of CRW to RW versus the ratio of driving amplitude to frequency. Here, we define all parameters in units of $\Omega_{\mathrm{e}2}$, $\Omega_{\mathrm{e}1}=2$. The order of the Bessel function is $n_t=1$, and the total particle size is $N=1$.

3. Adiabatic SR and SRS state preparation

Having discussed the engineering of the ADM, we now demonstrate that the tunable anisotropic parameter can facilitate the preparation of an adiabatic state with the nearest-neighbor Rydberg interaction. One method for preparing the ground state of complex systems is to adiabatically evolve from an easily accessible ground state. For Rydberg atom systems in optical cavities, the normal state can be chosen to be the initial ground state. We focus on the target ground states of the SR and SRS states, which both exist in the current ADM with the Rydberg atomic interaction.

Before delving into the impact of the CRW on the state preparation, we note that the Hamiltonian (17) remains invariant under the transformation $(a,a^{\dagger})\to(-a,-a^{\dagger})$ and $(\sigma_j^{-},\sigma_j^{+})\to(-\sigma_j^{-},-\sigma_j^{+})$. This provides the insight that there is one conserved quantity, i.e., parity, which is constructed as follows: $P=(-1)^{a^{\dagger}a}\prod_{j=1}^{N}\sigma_j^{z}$. Assuming the time-driven Hamiltonian retains parity symmetry throughout the whole evolution process, then one instantaneous eigenstate will always maintain fixed parity. According to recent research into

symmetry-protected quantum adiabatic evolution,[70] population transfer between different eigenstates with different parities is strictly forbidden; only state transitions of the same parity are allowed. The following discussion will exploit this principle.

We employ a Runge–Kutta method and exact diagonalization (ED) to simulate the adiabatic evolution. The Runge–Kutta method is utilized to evolve the wave function based on the instantaneous Hamiltonian, while ED is employed to obtain the eigenstates of the instantaneous Hamiltonian. For simplicity, the numerical simulation is conducted on a one-dimensional chain; however, the results are similarly applicable to a square lattice. Due to the exponential growth of the Hilbert space with the number of particles, we simulate the system with $N = 6$ atoms and a photon cutoff number of $N_a = 40$. During the process, we monitor various quantities: the fidelity $F = |\langle\psi(t)|\psi_e(t)\rangle|^2$ between the propagated state $\psi(t)$ and the instantaneous eigenstates $\psi_e(t)$, the mean number of cavity photons $N_a = a^\dagger a$, and the structural factor $S(q)/N = \langle|\sum_{j=1}^{N} P_j e^{iqr_j}|^2\rangle/N^2$ with $q = \pi$. Here N_a and $S(q)$ help us identify the characteristics of the eigenstates we care about.

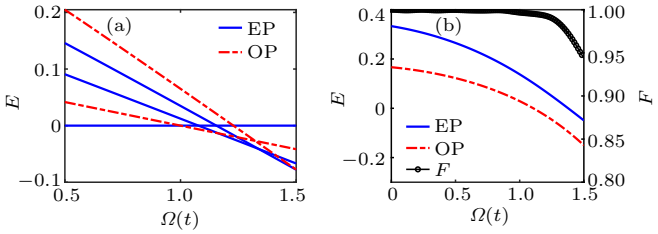


Fig. 3. (a) Low-energy spectrum as a function of coupling strength $\Omega(t)$ for $\alpha = 0$. (b) Low-energy spectrum and fidelity (black circles, denoted by F) versus $\Omega(t)$ for $\alpha = 0.7$. Here, the blue solid line and the red dot-dashed line represent even parity (EP) and odd parity (OP), respectively, corresponding to eigenvalues of the P operator of 1 and -1. For a unit Rydberg interaction strength V, we set $\widetilde{\omega}_C = 1$ and $\widetilde{\omega}_A = 1$. We retain the Hilbert space with a photon number of $N_a \leq 40$ and a lattice size of $N = 6$.

Figure 3 shows some instantaneous eigenenergies related to the SR state preparation, where the sweeping protocol chosen is $\Omega(t) = \Omega_F t/T_{SR}$. We set the required preparation time $T_{SR} \propto 20/V$ and the final coupling strength $\Omega_F = 1.5$ V in the numerical simulation. Experimentally, such a process can be achieved by gradually increasing the intensity of classical light. Due to the parity symmetry, the instantaneous eigenstates possess even or odd parity (see the corresponding blue solid line or the red dotted solid line in Fig. 3). When $\alpha = 0$, which implies that the CRW has vanished, one observes some energy level crossings of even-parity eigenstates in Fig. 3(a). Since the adiabatic evolution condition is violated in such cases, a target ground state with even parity can never be adequately adiabatically prepared from the initial even-parity ground state. With an increase in α, however, some gaps develop between those even-parity energy spectra, as shown in Fig. 3(b). Although quasi-degeneracy is evident at the final moment, $\Omega(T_{SR}) = \Omega_F$, the odd-parity instantaneous eigenstate is never occupied if one chooses the lowest-energy even-parity adiabatic route. In Fig. 3(b), we present the calculated fidelity for the entire instantaneous process, which clearly corroborates our discussion. Therefore, by tuning α, the adiabatic evolution condition can be satisfied and the SR state can be prepared.

Our discussion of the preparation of the SRS state proceeds similarly. Upon linearly sweeping $\widetilde{\omega}_A$ from 0.5 V to -0.1 V, an instantaneous low-energy spectrum appears, as shown in Fig. 4. The required preparation time is $T_{SRS} \propto 10/V$. We first focus on the limit $\alpha = 0$. Given that the initial ground state and the target state share the same even parity, the even-parity energy level crossing shown in Fig. 4(a) indicates that it is impossible to transfer to the SRS state with high fidelity through adiabatic evolution. Again, according to the principle of symmetry-protected transition, we now disregard the odd-parity eigenstates because of their different parity from the target state. Just as shown in Fig. 4(b), the level crossing can be avoided by opening a finite gap between the instantaneous eigenstates of even parity when increasing α. Then, adiabatic evolution always appears if our system is driven sufficiently slowly. Our numerical fidelity (black circles in Fig. 4(b)) demonstrates that most of the population stays in the instantaneous lowest-energy eigenstate of even parity, which indeed confirms our analysis. The fidelity curve further demonstrates that, under symmetry protection, the SRS state can be adiabatically evolved from the ground state of the normal phase with higher fidelity compared to the SR phase.

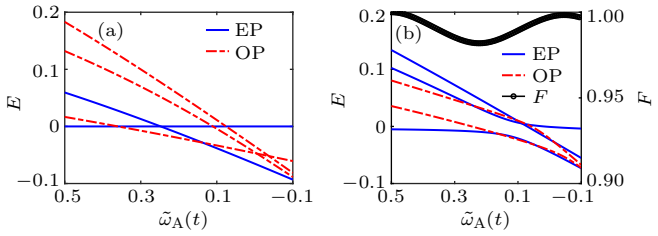


Fig. 4. (a) Dependence of the low-energy spectrum on $\widetilde{\omega}_A(t)$ for $\alpha = 0$. (b) Dependence of the low-energy spectrum on $\widetilde{\omega}_A(t)$ for $\alpha = 0.3$. The right-hand y-axis of part (b) represents the fidelity (F, black circles), which is the degree of overlap of the propagated state and the first even-parity instantaneous eigenstates. Even parity (EP) and odd parity (OP) are represented by the blue solid line and the red dotted solid line, respectively. For other parameters, we set $V = 1$, $\Omega = 0.6$, and $\widetilde{\omega}_C = 1$.

In summary, we can regulate the distribution of instantaneous eigenenergies by tuning the anisotropic parameter α, thus facilitating the preparation of the SR and SRS states. In particular, by employing the principle of symmetry-protected transitions, our tuning strategy aims to reject eigenstates with the same parity as the target adiabatic pathway while ensuring that the eigenstates close to the pathway have different parity. In this way, roughly speaking, the efficiency of adiabatic state

preparation is determined by the energy gap between the nearest neighboring instantaneous eigenstates of the same parity.

4. Conclusions and outlook

In this paper, we reported the design and Floquet engineering of an anisotropic Dicke model based on Rydberg arrays in a cavity. We also demonstrated the possibility of manipulating the anisotropic parameter which determines the ratio of CRW to RW states by appropriately adjusting the driving microwave field. As an example, our adiabatic evolution results elucidate a superior control strategy for synthesizing complex quantum states from simpler ones. This level of control is not only crucial for tailoring the behavior of the system in a targeted manner but also has great potential for applications even beyond the realm of physics, for instance, combinatorial optimization problems.[58,59]

Acknowledgements

This work was supported by the National Natural Science Foundation of China (Grant No. 12274045). T.W. acknowledges funding from the National Natural Science Foundation of China (Grant No. 12347101) and the Program of the State Key Laboratory of Quantum Optics and Quantum Optics Devices (Grant No. KF202211).

References

[1] Kockum A F, Miranowicz A, De Liberato S, Savasta S and Nori F 2019 *Nat. Rev. Phys.* **1** 19
[2] Gutzler R, Garg M, Ast C R, Kuhnke K and Kern K 2021 *Nat. Rev. Phys.* **3** 441
[3] Dicke R H 1954 *Phys. Rev.* **93** 99
[4] Agarwal S, Rafsanjani S M H and Eberly J H 2012 *Phys. Rev. A* **85** 043815
[5] Fink J M, Bianchetti R, Baur M, Göppl M, Steffen L, Filipp S, Leek P J, Blais A and Wallraff A 2009 *Phys. Rev. Lett.* **103** 083601
[6] Restrepo J and Rodríguez B A 2016 *J. Phys. B: Atom. Mol. Opt. Phys.* **49** 125502
[7] Feng M, Zhong Y P, Liu T, Yan L L, Yang W L, Twamley J and Wang H 2015 *Nat. Commun.* **6** 7111
[8] Yang H Y, Shi H L, Wan Q K, Zhang K, Wang X H and Yang W L 2024 *Phys. Rev. A* **109** 012204
[9] Fujii K 2014 arXiv:1301.3585
[10] Garbe L, Egusquiza I L, Solano E, Ciuti C, Coudreau T, Milman P and Felicetti S 2017 *Phys. Rev. A* **95** 053854
[11] Liberti G and Zaffino R 2005 *Euro. Phys. J. B* **44** 535
[12] Forn-Diaz P, Lamata L, Rico E, Kono J and Solano E 2019 *Rev. Mod. Phys.* **91** 025005
[13] Jaako T, Xiang Z L, Garcia-Ripoll J J and Rabl P 2016 *Phys. Rev. A* **94** 033850
[14] Kirton P, Roses M M, Keeling J and Dalla Torre E G 2019 *Advanced Quantum Technologies* **2** 1800043
[15] Baumann K, Guerlin C, Brennecke F and Esslinger T 2010 *Nature* **464** 1301
[16] Chiacchio E I R, Nunnenkamp A and Brunelli M 2023 *Phys. Rev. Lett.* **131** 113602
[17] Das P, Wüster S and Sharma A 2024 *Phys. Rev. A* **109** 013715
[18] Garraway B M 2011 *Phil. Tran. Roy. Soc. A Math. Phys. Eng. Sci.* **369** 1137
[19] Hassan S, Hildren G, Puri R and Bullough R 1982 *J. Phys. B: Atom. Mol. Opt. Phys.* **15** 2635
[20] Niemczyk T, Deppe F, Huebl H, Menzel E P, Hocke F, Schwarz M J, Garcia-Ripoll J J, Zueco D, Huemmer T, Solano E, Marx A and Gross R 2010 *Nat. Phys.* **6** 772
[21] Cao X, You J Q, Zheng H, Kofman A G and Nori F 2010 *Phys. Rev. A* **82** 022119
[22] Garziano L, Stassi R, Macrì V, Kockum A F, Savasta S and Nori F 2015 *Phys. Rev. A* **92** 063830
[23] Wang X, Miranowicz A, Li H R and Nori F 2016 *Phys. Rev. A* **94** 053858
[24] Casanova J, Romero G, Lizuain I, García-Ripoll J J and Solano E 2010 *Phys. Rev. Lett.* **105** 263603
[25] Wang X, Miranowicz A, Li H R and Nori F 2017 *Phys. Rev. A* **96** 063820
[26] Liu M, Chesi S, Ying Z J, Chen X, Luo H G and Lin H Q 2017 *Phys. Rev. Lett.* **119** 220601
[27] Ashhab S and Nori F 2010 *Phys. Rev. A* **81** 042311
[28] Ma K K W and Law C K 2015 *Phys. Rev. A* **92** 023842
[29] Le Boité A, Hwang M J, Nha H and Plenio M B 2016 *Phys. Rev. A* **94** 033827
[30] Hwang M J, Kim M S and Choi M S 2016 *Phys. Rev. Lett.* **116** 153601
[31] Hioe F T 1973 *Phys. Rev. A* **8** 1440
[32] de Aguiar M A M, Furuya K and Nemes M C 1991 *Quantum Optics* **3** 305
[33] Bastarrachea-Magnani M A, Lerma-Hernández S and Hirsch J G 2016 *J. Stat. Mech.: Theor. Exp.* **2016** 093105
[34] Aedo I and Lamata L 2018 *Phys. Rev. A* **97** 042317
[35] Das P, Bhakuni D S and Sharma A 2023 *Phys. Rev. A* **107** 043706
[36] Zhu X, Lü J H, Ning W, Shen L T, Wu F and Yang Z B 2024 *Phys. Rev. A* **109** 052621
[37] Das P, Bhakuni D S, Santos L F and Sharma A 2023 *Phys. Rev. A* **108** 063716
[38] Buijsman W, Gritsev V and Sprik R 2017 *Phys. Rev. Lett.* **118** 080601
[39] Georgescu I M, Ashhab S and Nori F 2014 *Rev. Mod. Phys.* **86** 153
[40] Altman E, Brown K R, Carleo G, Carr L D, Demler E, Chin C, DeMarco B, Economou S E, Eriksson M A, Fu K M C, Greiner M, Hazzard K R, Hulet R G, Kollár A J, Lev B L, Lukin M D, Ma R, Mi X, Misra S, Monroe C, Murch K, Nazario Z, Ni K K, Potter A C, Roushan P, Saffman M, Schleier-Smith M, Siddiqi I, Simmonds R, Singh M, Spielman I, Temme K, Weiss D S, Vučković J, Vuletić V, Ye J and Zwierlein M 2021 *PRX Quantum* **2** 017003
[41] Daley A J, Bloch I, Kokail C, Flannigan S, Pearson N, Troyer M and Zoller P 2022 *Nature* **607** 667
[42] Browaeys A, Barredo D and Lahaye T 2016 *J. Phys. B: Atom. Mol. Opt. Phys.* **49** 152001
[43] Saffman M 2016 *J. Phys. B: Atom. Mol. Opt. Phys.* **49** 202001
[44] Zhang Z Y, Ding D S and Shi B S 2021 *Chin. Phys. B* **30** 020307
[45] Wu X, Liang X, Tian Y, Yang F, Chen C, Liu Y C, Tey M K and You L 2021 *Chin. Phys. B* **30** 020305
[46] Han Y and Yi W 2024 *Chin. Phys. Lett.* **41** 033201
[47] Solookinejad G, Jabbari M, Nafar M, Sangachin E A and Asadpour S H 2019 *International Journal of Theoretical Physocs* **58** 1359
[48] Parigi V, Bimbard E, Stanojevic J, Hilliard A J, Nogrette F, Tualle-Brouri R, Ourjoumtsev A and Grangier P 2012 *Phys. Rev. Lett.* **109** 233602
[49] Lin G W, Qi Y H, Lin X M, Niu Y P and Gong S Q 2015 *Phys. Rev. A* **92** 043842
[50] Boddeda R, Usmani I, Bimbard E, Grankin A, Ourjoumtsev A, Brion E and Grangier P 2016 *J. Phys. B: Atom. Mol. Opt. Phys.* **49** 084005
[51] Guerlin C, Brion E, Esslinger T and Mølmer K 2010 *Phys. Rev. A* **82** 053832
[52] Grinkemeyer B, Guardado-Sanchez E, Dimitrova I, Shchepanovich D, Mandopoulou G E, Borregaard J, Vuletić V and Lukin M D 2025 *Science* **387** 1301
[53] Li R, He S, Meng Z J, Jin Z and Gong W J 2023 *Chin. Phys. Lett.* **40** 060302
[54] Ebadi S, Wang T T, Levine H, Keesling A, Semeghini G, Omran A, Bluvstein D, Samajdar R, Pichler H, Ho W W, Choi S, Sachdev S, Greiner M, Vuletic V and Lukin M D 2021 *Nature* **595** 227

[55] Bluvstein D, Omran A, Levine H, Keesling A, Semeghini G, Ebadi S, Wang T T, Michailidis A A, Maskara N, Ho W W, Choi S, Serbyn M, Greiner M, Vuletic V and Lukin M D 2021 *Science* **371** 1355
[56] Manovitz T, Li S H, Ebadi S, Samajdar R, Geim A A, Evered S J, Bluvstein D, Zhou H, Koyluoglu N U, Feldmeier J, Dolgirev P E, Maskara N, Kalinowski M, Sachdev S, Huse D A, Greiner M, Vuletic V and Lukin M D 2025 *Nature* **638** 86
[57] Ding D, Bai Z, Liu Z, Shi B, Guo G, Li W and Adams C S 2024 *Science Advances* **10** eadl5893
[58] Nguyen M T, Liu J G, Wurtz J, Lukin M D, Wang S T and Pichler H 2023 *PRX Quantum* **4** 010316
[59] Bombieri L, Zeng Z, Tricarico R, Lin R, Notarnicola S, Cain M, Lukin M D and Pichler H 2024 arXiv:2411.04645
[60] Puel T O and Macrì T 2024 *Phys. Rev. Lett.* **133** 106901
[61] Rohn J, Hörmann M, Genes C and Schmidt K P 2020 *Phys. Rev. Res.* **2** 023131
[62] Zhang X F, Sun Q, Wen Y C, Liu W M, Eggert S and Ji A C 2013 *Phys. Rev. Lett.* **110** 090402
[63] An G Q, Zhou Y H, Wang T and Zhang X F 2022 *Phys. Rev. B* **106** 195435
[64] Gelhausen J, Buchhold M, Rosch A and Strack P 2016 *SciPost Phys.* **1** 004
[65] Liu W, Zhang L and Wang T 2023 *Chin. Phys. B* **32** 053203
[66] Lu X T, Wang T, Li T, Zhou C H, Yin M J, Wang Y B, Zhang X F and Chang H 2021 *Phys. Rev. Lett.* **127** 033601
[67] Bravyi S, DiVincenzo D P and Loss D 2011 *Annals of Physics* **326** 2793
[68] Nevado P and Porras D 2015 *Phys. Rev. A* **92** 013624
[69] Gammelmark S and Mølmer K 2011 *New J. Phys.* **13** 053035
[70] Zhuang M, Huang J, Ke Y and Lee C 2020 *Annalen der Physik* **532** 2070020